Proc. of the European Safety and Reliability Conference (ESREL 2026)
Edited by José C. Matos, Paulo B. Lourenço, Michael Beer, Daniel Oliveira,
Edoardo Patelli, Hélder S. Sousa, Rui A. Silva and Monica Santamaria
 Published by Research Publishing, Singapore.
doi: 10.3850/ESREL2026061419_esrel26-p26417-cd

A PHYSICS-INFORMED NEURAL NETWORK-BASED METHOD FOR RELIABILITY ANALYSIS OF STOCHASTIC DEGRADATION SYSTEMS

Xiwen Xie*
University of Science and Technology of China, Hefei. E-mail: xw03@mail.ustc.edu.cn
Changzheng Yin
University of Science and Technology of China, Hefei. E-mail: yinchangzheng@mail.ustc.edu.cn
Changhong Peng
University of Science and Technology of China, Hefei. E-mail: pengch@ustc.edu.cn

Abstract

This study presents a reliability analysis method for stochastic degradation systems using a physics-informed neural network (PINN). The system degradation process is modelled by continuous diffusion-type stochastic differential equations. Based on stochastic differential theory, the reliability problem is transformed into solving the governing equation of the probability density function of the degradation state, such as the Fokker–Planck equation. A loss function is constructed by embedding these physical constraints into the deep learning framework, enabling the PINN to solve the forward problem efficiently. The proposed approach is validated through numerical examples involving Wiener and Ornstein–Uhlenbeck processes. The results demonstrate good agreement between the PINN-based solutions and Monte Carlo simulations, indicating that the proposed method offers a promising alternative for computationally intensive reliability analyses.

Keywords: Stochastic differential equations, PINN, reliability analysis.

1. Introduction

The safe and reliable operation of complex modern industrial systems, spanning aerospace, nuclear power, high-speed rail, and precision manufacturing, critically depends on the accurate characterization of component degradation processes and the precise prediction of remaining useful life. System failures are broadly categorized into sudden "hard failures" from extreme loads and gradual "soft failures" from cumulative performance deterioration (Fan et al., 2017). With the widespread adoption of sensor networks and Condition Monitoring Systems (CMS), modeling degradation for soft failure has become central to real-time reliability assessment. Current research in this domain is primarily structured around three distinct modeling paradigms: methods based on physical mechanisms (Physics-of-Failure, PoF), those founded on statistical stochastic processes, and hybrid approaches that integrate both (Shahraki et al., 2017). PoF methods, grounded in damage mechanics, construct deterministic models from first principles, such as the Paris' law for fatigue crack growth (Paris et al., 1963). While offering strong physical interpretability, they often struggle to account for the inherent randomness observed in real-world conditions due to material heterogeneity and environmental noise. Consequently, stochastic process models have gained prominence for their ability to formally quantify uncertainty (Zhang et al., 2021). Widely used frameworks include the Wiener process for non-monotonic degradation (Zhai et al., 2017), the Gamma process for monotonic accumulation (Wei et al., 2014), and the Inverse Gaussian or Fractional Brownian Motion for more complex scenarios with random effects or long-range dependence (Ye et al., 2014).

Despite their utility, traditional stochastic and hybrid models face significant mathematical and computational bottlenecks that limit their application to modern, complex systems. A core challenge lies in the inherent trade-off between model flexibility and analytical tractability. While models like the linear Wiener process benefit from closed-form solutions for key reliability metrics like the First-Passage Time (FPT) distribution, this analytical convenience comes at the cost of restrictive assumptions, such

as stationary independent increments and linear drift. Real-world degradation, however, is often non-linear, non-stationary, and influenced by multiple coupled covariates, rendering these simple models inadequate. For more flexible, non-linear stochastic differential equation (SDE) models, analytical solutions are generally unavailable (Iannacone & Gardoni, 2024). The conventional alternative—numerically solving the governing Fokker–Planck equation (FPE) for the probability density function (PDF) using grid-based discretization schemes such as the finite element method—is constrained by the curse of dimensionality, which renders it computationally intractable for systems with high-dimensional state spaces. Similarly, Monte Carlo (MC) simulation remains computationally prohibitive for real-time prognostics due to the millions of trajectories required to estimate low failure probabilities (Zhai et al., 2022).

A promising paradigm shift is emerging with the advent of Physics-Informed Neural Networks (PINNs). This novel framework seamlessly integrates the flexibility of deep learning with the rigor of physical laws by directly embedding governing equations, such as the FPE, into the neural network's loss function (He et al., 2025). This approach offers two advantages for reliability analysis. First, it liberates the modeler from restrictive pre-specified statistical forms, enabling the handling of complex, non-linear, and state-dependent degradation dynamics while maintaining strict adherence to the underlying physics (Liu et al., 2022). Second, PINNs provide a "mesh-free" pathway to obtain the full evolution of the degradation PDF. Unlike traditional grid-based schemes, where computational costs grow exponentially with dimensionality, PINN complexity is primarily governed by network architecture and sampling strategies. This generally enables better scalability in problems with 3-6 dimensions (Karniadakis et al., 2021). Once trained, the network can directly predict the PDF at any spatiotemporal point, bypassing the need for costly MC simulations (Habibollahi et al., 2023).

However, a significant methodological disparity persists in the field of reliability engineering. For systems described by discrete states, a mature and standardized framework exists based on Markov Chain theory, offering efficient analytical and numerical solutions supported by established engineering tools (Zhou et al. 2023). In stark contrast, for systems with continuous degradation paths, there is a notable lack of a unified, systematic computational methodology. This study seeks to bridge this methodological gap by synthesizing current degradation modeling approaches, with a focus on the potential of PINN to mitigate certain limitations inherent in conventional stochastic models.

2. Method

2.1. *SDE-based deterioration modelling*

To enhance modelling flexibility and unification, stochastic differential equations are introduced as the mathematical foundation of such approaches. By integrating deterministic evolutionary trends with random perturbations, SDEs inherently represent solutions as stochastic processes, making them an ideal choice for simulating complex real-world phenomena. A general SDE can be expressed in the form:

$$dX(t) = \mu(X,t)dt + \sigma(X,t)dB(t) \tag{1}$$

where, $X(t)$ is the stochastic process of interest, $\mu(X,t)$ is the drift coefficient, $\sigma(X,t)$ is the diffusion coefficient, $B(t)$ is a standard Brownian motion.

Equation (1) can be extended to include jump-type processes:

$$dX(t) = \mu(X,t)\,dt + \sigma(X,t)\,dB_t + \int_{\mathbb{R}} \gamma(X,t,z)N(dt,dz) \tag{2}$$

where, the integral term represents the jump term contribution under the Lévy measure; $\gamma(X,t,z)$ and $N(dt,dz)$ are the magnitude and number of discontinuous jumps, respectively.

Table 1. Special cases of stochastic processes and corresponding SDE forms

Stochastic Process	SDE Form	Deterioration path
Wiener Process	$dX(t) = \mu dt + \sigma dB(t)$	Continuous
Ornstein–Uhlenbeck	$dX(t) = \theta(\mu - X)dt + \sigma dB(t)$	Continuous
Gamma Process	$dX(t) = \alpha dt + \beta dJ(t)$	Discontinuous
Poisson Process	$dX(t) = \lambda dt + dP(t)$	Discontinuous

Table 1 lists some special cases of stochastic processes and their corresponding SDE forms. This study primarily focuses on stochastic processes with continuous deterioration paths.

2.2. *Problem formulation*

Based on this general SDE framework, the corresponding Fokker–Planck (F-P) equation for the probability density $p(x,t)$ can be derived using Itô's Lemma (Iannacone & Gardoni, 2024):

$$\frac{\partial p(x,t)}{\partial t} = -\frac{\partial}{\partial x}\left[\mu(x,t)p(x,t)\right] + \frac{1}{2}\frac{\partial^2}{\partial x^2}\left[\sigma^2(x,t)p(x,t)\right] \tag{3}$$

Therefore, the reliability assessment problem is equivalently formulated as solving the F-P equation under appropriate initial and boundary conditions, where the survival probability corresponds to the integral of the probability density over the safe domain, as shown in Fig. 1.

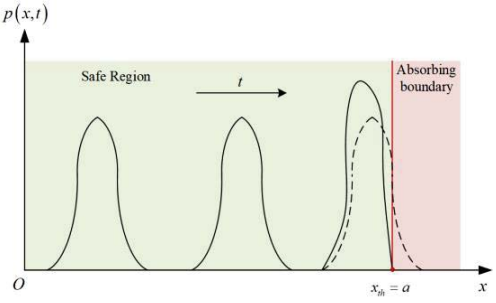

Fig. 1. Schematic diagram showing the probability density evolution within the safe region.

For different systems, the drift and diffusion coefficients often have significantly different dimensions. To unify the problem formulation, the original problem can be non-dimensionalized following the method introduced in **Appendix A**, which is equivalent to solving the Fokker-Planck equation on a new rectangular domain.

After non-dimensionalization, the probability density distribution of the degradation quantity satisfies Eq. (4).

$$\begin{cases} \dfrac{\partial \tilde{p}(\xi,\tau)}{\partial \tau} = -\dfrac{\partial}{\partial \xi}\left[\tilde{\mu}(\xi,\tau)\tilde{p}(\xi,\tau)\right] + \dfrac{1}{2}\dfrac{\partial^2}{\partial \xi^2}\left[\tilde{\sigma}^2(\xi,\tau)\tilde{p}(\xi,\tau)\right] \\ \tilde{p}(\xi,0) = \delta(\xi = \xi_0),\ \tilde{p}(0,\tau) = \tilde{p}(1,\tau) = 0 \end{cases} \tag{4}$$

Where, $\tilde{p}(\xi,\tau), \tilde{\mu}(\xi,\tau), \tilde{\sigma}^2(\xi,\tau)$ are the transformed PDF, drift coefficient, and diffusion coefficient, respectively. $\delta(\bullet)$ is the Dirac delta function. A narrow Gaussian distribution is commonly used to approximate this function.

2.3. *PINN-based reliability analysis*

The PINN framework represents a paradigm shift in solving partial differential equations (PDEs) like F-P equations by seamlessly integrating deep learning with physical laws. At its core, PINN employs a deep neural network (DNN) as a universal function approximator to represent the solution $\tilde{p}(\xi,\tau)$ of Eq. (4), as shown in Fig. 2.

The PINN is trained to satisfy the PDE, the initial condition, and the boundary conditions simultaneously, which is achieved by constructing a composite loss function:

$$\mathcal{L}_{total} = \lambda_{PDE}\mathcal{L}_{PDE} + \lambda_{IC}\mathcal{L}_{IC} + \lambda_{BC}\mathcal{L}_{BC} \tag{5}$$

$$\mathcal{L}_{PDE} = \frac{1}{N_r}\sum_{i=1}^{N_r}\left|\mathcal{R}(\xi^i,\tau^i)\right|^2,$$

$$\mathcal{R}(\xi^i,\tau^i) = \left(\frac{\partial \tilde{p}}{\partial \tau} + \frac{\partial}{\partial \xi}\left[\tilde{\mu}(\xi,\tau)\tilde{p}\right] - \frac{1}{2}\frac{\partial^2}{\partial \xi^2}\left[\tilde{\sigma}^2(\xi,\tau)\tilde{p}\right]\right)\Bigg|_{\xi=\xi^i,\tau=\tau^i} \tag{6}$$

$$\mathcal{L}_{IC} = \frac{1}{N_o}\sum_{i=1}^{N_o}\left|p(\xi^i,0) - \delta(\xi^i)\right|^2 \tag{7}$$

$$\mathcal{L}_{BC} = \frac{1}{2N_b}\sum_{i=1}^{N_b}\left(\left|\tilde{p}(0,\tau^i)\right|^2 + \left|\tilde{p}(1,\tau^i)\right|^2\right) \tag{8}$$

where, $\mathcal{L}_{PDE}$ penalizes the PDE residual at N_r sample points in the interior of the domain; $\mathcal{L}_{IC}$ enforces the initial condition at N_o sample points when $\tau = 0$; $\mathcal{L}_{BC}$ enforces the boundary conditions at N_b sample points over the time interval. The coefficients $\{\lambda_{PDE}, \lambda_{IC}, \lambda_{BC}\}$ balance the contribution of each term.

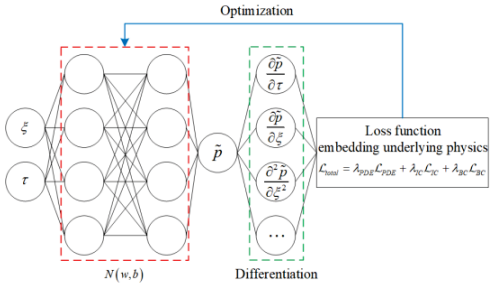

Fig. 2. The structure of proposed PINN model.

A key advantage of PINNs is the use of automatic differentiation (AD) to compute

derivatives of $\tilde{p}(\xi,\tau)$ with respect to ξ and τ exactly, avoiding discretization errors inherent in traditional numerical methods. The parameters $\{w,b\}$ of DNN model are optimized via gradient descent to minimize $\mathcal{L}_{total}$, effectively solving the PDE in a forward manner without relying on conventional grid-based solvers. However, a central challenge arises because this loss function combines terms of vastly differing scales—such as PDE residuals, initial conditions, and boundary conditions—often leading to unstable training and unphysical solutions as optimization disproportionately favors dominant terms. To address this imbalance, we employed an adaptive weighting strategy based on Neural Tangent Kernel (NTK) theory, which dynamically balances the loss components by adjusting their weights inversely according to associated NTK eigenvalues. The detailed algorithm can be found in Wang's work (Wang et al., 2022).

In reliability analysis for degradation processes, the governing Fokker-Planck equation can be naturally embedded into the PINN loss function. This formulation enables the direct, sampling-free recovery of the time-varying probability density function (PDF), which is essential for evaluating time-dependent system reliability. The reliability can be computed by Eq. (9).

$$R(t)=P\left(X(t)<a\right)=\int_0^a p(x,t)dx \tag{9}$$

where a denotes the failure threshold of degradation, serving as an absorbing boundary for probability transition, as illustrated in Fig. 1.

3. Case study

To illustrate the effectiveness of the proposed method, two classical stochastic processes are considered: a linear Wiener process and an Ornstein-Uhlenbeck (OU) process. Subsection 3.1 analyses a battery degradation problem governed by a linear Wiener process, while Subsection 3.2 examines a cable thermal aging case described by an OU process.

3.1. Battery Performance Deterioration (Wiener process)

Based on the findings in (Zhu et al., 2022), the capacity degradation of Nickel-Manganese-Cobalt (NMC) Lithium-ion cells approximately follows a linear Wiener process as expressed in Eq. (10). The estimated coefficients are $(\mu,\sigma)=(9.592,5.862)$. The initial capacity of the battery is 2525 mAh, and a cell is considered failed when its capacity degrades below the threshold of 1875 mAh. The mission time for this case is set to 400 cycles.

$$dX(t)=\mu dt+\sigma dB(t) \tag{10}$$

Were, $dX(t)$ is the capacity loss, $B(t)$ is a standard Brownian motion.

Table 2 details the parameter configurations for the PINN model. The network architecture employs a fully connected neural network comprising three hidden layers. The training batch size is defined by the number of random sampling points used to enforce physical constraints: 300 points for both the initial condition and PDE residual, along with 150 points for each of the two boundaries.

Table 2. PINN model parameters.

Category	Parameter	Value
Network	layers	[2, 128, 128, 128, 1]
	Activation	tanh
	Weight initialization	Xavier
Training	Iterations	40,000
	Batch size	300
	Initial learning rate	0.0001
	Learning rate decay	0.9/1000 iterations
	Optimizer	Adam

Figure 3 depicts the convergence history of each loss component. Training is terminated via early stopping once the loss stabilizes, which occurs around 40,000 iterations. Figure 4 presents the PDF obtained from PINN model, alongside the absolute error between PINN prediction and analytical solution. For the linear Wiener process with a fixed absorbing boundary, the PDF admits a closed-form expression given in Eq. (11). The relative error between the PINN result and the analytical solution, computed via Eq. (12), is 5.5×10^{-3}, indicating good agreement.

$$p(x,t)=\frac{1}{\sigma\sqrt{2\pi t}}\left(\exp\left(-\frac{(x-\mu t)^2}{2\sigma^2 t}\right)-\exp\left(\frac{2\mu a}{\sigma^2}-\frac{(x-2a-\mu t)^2}{2\sigma^2 t}\right)\right) \tag{11}$$

$$E_{L_2} = \frac{\sqrt{\sum_{i=1}^{N}\sum_{j=1}^{N}\left(\tilde{p}_{Analytical}\left(\xi_i,\tau_j\right)-\tilde{p}_{PINN}\left(\xi_i,\tau_j\right)\right)^2}}{\sqrt{\sum_{i=1}^{N}\sum_{j=1}^{N}\left(\tilde{p}_{Analytical}\left(\xi_i,\tau_j\right)\right)^2}} \quad (12)$$

Here, E_{L_2} is the vector-based relative $L2$ error (Sahin et al., 2024) between PINN predictions and true values, where the test points are sampled from a uniform grid.

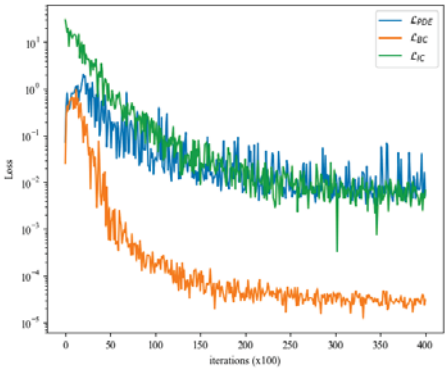

Fig. 3. Contribution of each loss term versus training iterations.

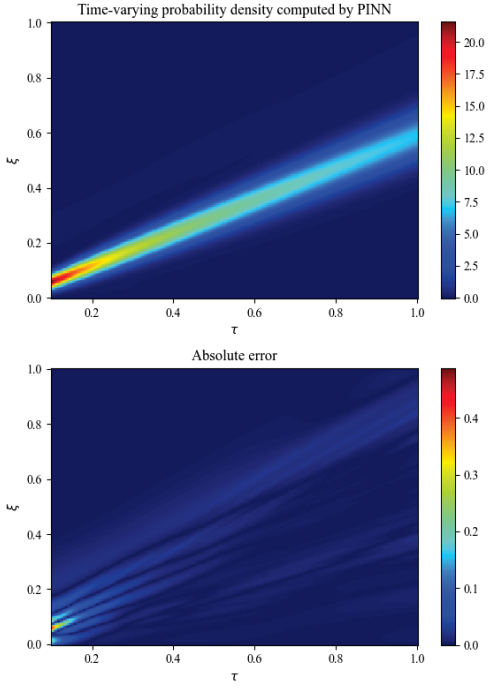

Fig. 4. Heatmap of $\tilde{p}(\xi,\tau)$ (top); Heatmap of the absolute error $\left|\tilde{p}_{PINN}-\tilde{p}_{Analytical}\right|$ (bottom).

3.2. Thermal aging of cables (OU process)

In nuclear power industry, the reliability of electrical cables is a critical safety concern. Cables in nuclear environments are continuously exposed to high temperatures and ionizing radiation, which lead to the degradation of insulation materials. A key degradation indicator is the elongation-at-break (EAB), which measures the ductility of the insulation. Figure 7.1 in NEUP report (Mosleh et al., 2019) indicates the decay rate is 0.57 per year under experimental condition of 80°C and a dose rate of 3 Gy/h. The initial EAB of the cable insulation sample is 558.6%. Failure is defined when the EAB degrades below 50%. The normalized EAB reduction, defined as X = 1-EAB*, is adopted as the degradation quantity. This measure asymptotically approaches a long-term mean of unity, reflecting the progressive embrittlement of the insulation material. Under a small-fluctuation assumption (i.e., $\sigma/\sqrt{2\lambda} \le 0.1$), the thermal aging process can be effectively represented by the following OU process:

$$dX(t) = \lambda(1-X)dt + \sigma dB(t) \quad (13)$$

Where, λ is the decay rate, σ is the diffusion coefficient.

Given lack of detailed uncertainty information for the actual degradation process, the upper bound of small-fluctuation condition is adopted as the diffusion coefficient (i.e., $\sigma = 0.11$). The total mission time of cables is set to four years. For Eq. (13), an analytical solution exists only for the free-boundary case (i.e., without absorbing boundary). However, an absorbing boundary must be introduced to represent the failure threshold in practical degradation scenarios, necessitating a numerical approach. The PINN configuration remains consistent with the settings summarized in Table 2. Figure 5 and Figure 6 present the convergence behaviour of the loss function and the PDF obtained from PINN model, respectively. To demonstrate that the PINN method is equally effective for such problems, comparative analyses were carried out against independent numerical benchmarks.

Appendix B outlines the Monte Carlo simulation (MCS) algorithm employed for verification, in which 40,000 samples were generated to ensure statistical stability. For the free-boundary case, the PDF of the OU

degradation process is given analytically by Eq. (14). Substituting this expression into Eq. (9) yields the time-dependent reliability of the cable insulation. Additionally, a finite-difference (FD) scheme was implemented as a further numerical reference. The method discretizes the spatial domain using a uniform grid, approximates the partial derivatives via central differences, and reduces the Fokker-Planck equation to a system of ordinary differential equations, which is then integrated forward in time. NDSolve[] in Mathematica was utilized to perform the FD computation. The results presented in Fig. 7 demonstrate strong agreement between the PINN predictions and the MC reference solutions, with a Root Mean Square Error (RMSE) of 0.0068. The free-boundary condition permits degradation paths to fluctuate back below the threshold after crossing it, which accounts for the higher reliability estimate relative to the absorbing-boundary results in Fig. 7.

$$p(x,t)=\sqrt{\frac{\lambda}{\pi\sigma^2(1-e^{-2\lambda t})}}\exp\left(-\frac{\lambda\left(a-1-(x_0-1)e^{-\lambda t}\right)^2}{\sigma^2\left(1-e^{-2\lambda t}\right)}\right) \tag{14}$$

Table 3 compares the computational time required by each method. Similar to FD method, a pre-trained PINN allows rapid pointwise evaluation, particularly when compared to MCS method, thereby showing potential for efficient reliability assessment in practical applications.

Table 3. Computational cost in Example 3.2 (Unit: s)

PINN training time	PINN prediction time	MCS method	Finite difference method
321	0.012	340	0.097

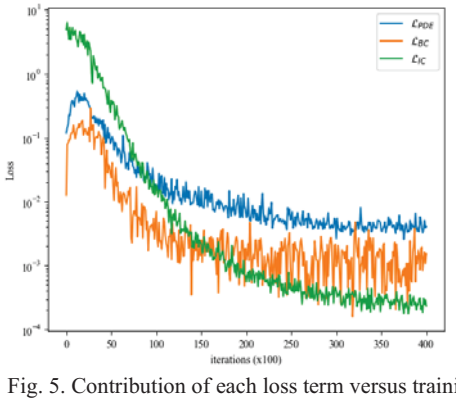

Fig. 5. Contribution of each loss term versus training iterations.

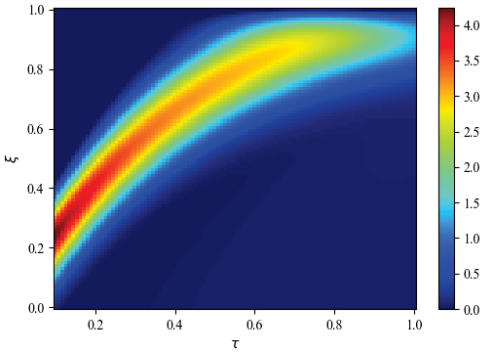

Fig. 6. Time-varying probability density $\tilde{p}(\xi,\tau)$ computed by PINN

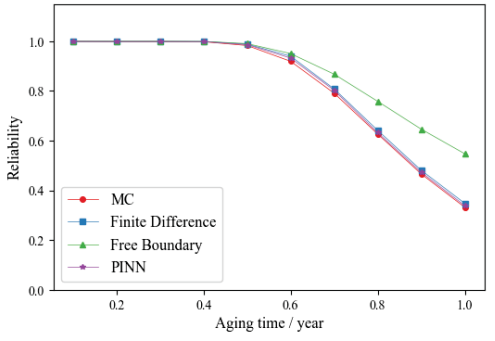

Fig. 7. Cable reliability calculated by different methods

4. Conclusions and discussion

This study has developed a reliability analysis framework for stochastic degradation systems by integrating PINNs with stochastic differential theory. The method directly solves the governing Fokker–Planck equation through the embedded physical constraints, avoiding costly sampling while preserving the mathematical structure of the underlying diffusion processes. Numerical validations based on both linear Wiener and mean-reverting Ornstein–Uhlenbeck degradation models demonstrate that the PINN solutions achieve high agreement with reference solutions, confirming both computational accuracy and physical consistency.

Although the current study focuses on the two-dimensional cases, PINN models offer a scalable alternative for higher-dimensional reliability analysis. Future work will extend this methodology to multi-dimensional degradation involving coupled covariates, potentially leveraging adaptive refinement sampling (Wu et

al., 2023) or operator learning (Lu et al., 2021). These advanced architectures are specifically designed to preserve numerical accuracy and computational efficiency as the complexity of the state space increases. Furthermore, in addition to continuous degradation, system reliability may be subject to shock loads (e.g., earthquakes). In such scenarios, the degradation process is governed by more complex stochastic differential equations, such as the Kolmogorov forward equation. Consequently, further improvements to the PINN model are required to address these more general problems.

Acknowledgement

This work is supported by the Open Fund of State Key Laboratory of Nuclear Power Safety Technology and Equipment (007-EC-B-2026-C76-P.T.30-02903).

Appendix A. Non-dimensionalization of the Fokker–Planck equation

The general one-dimensional Fokker–Planck equation is given by Eq. (A.1).

$$\frac{\partial}{\partial t}p(x,t) = -\frac{\partial}{\partial x}\left[A(x,t)\,p(x,t)\right] + \frac{\partial^2}{\partial x^2}\left[B(x,t)\,p(x,t)\right] \tag{A.1}$$

where, $A(x,t)$ is the drift coefficient, $B(x,t)$ is the diffusion coefficient, and both are sufficiently smooth within the domain.

Consider the linear scaling transformation:

$$L_x \triangleq x_{\max} - x_{\min}, L_t \triangleq T_{\max} - T_{\min}$$

$$x = x_{\min} + L_x\xi, t = T_{\min} + L_t\tau, (\xi,\tau) \in [0,1]\times[0,1] \tag{A.2}$$

To ensure that the probability remains normalized to 1 on the unit square domain, a Jacobian rescaling must be introduced:

$$\tilde{p}(\xi,\tau) = L_x\,p(x_{\min} + L_x\xi, T_{\min} + L_t\tau)$$

$$p(x,t) = \frac{1}{L_x}\tilde{p}\left(\frac{x - x_{\min}}{L_x}, \frac{t - T_{\min}}{L_t}\right) \tag{A.3}$$

where, $\tilde{p}(\xi,\tau)$ is the probability density on the unit square domain and $p(x,t)$ is the probability density on the original domain.

Due to the smoothness of the coefficients, the following composite mapping can be performed on the unit square domain:

$$\begin{cases} \tilde{A}(\xi,\tau) = \dfrac{L_t}{L_x}A\left(x_{\min} + L_x\xi, T_{\min} + L_t\tau\right) \\ \tilde{B}(\xi,\tau) = \dfrac{L_t}{L_x^2}B\left(x_{\min} + L_x\xi, T_{\min} + L_t\tau\right) \end{cases} \tag{A.4}$$

Thus, the general F-P equation on the unit square domain is obtained as:

$$\frac{\partial}{\partial\tau}\tilde{p}(\xi,\tau) = -\frac{\partial}{\partial\xi}\left[\tilde{A}(\xi,\tau)\tilde{p}(\xi,\tau)\right] + \frac{\partial^2}{\partial\xi^2}\left[\tilde{B}(\xi,\tau)\tilde{p}(\xi,\tau)\right] \tag{A.5}$$

Solving Eq. (A.5) and substituting the result back into Eq. (A.3) yields the probability density function within the original domain.

Equation (A.5) indicates that the general form of the Fokker–Planck equation is closed under linear scaling $(x,t) \mapsto (\xi,\tau) \in [0,1]^2$. The structure of the equation is preserved in the F-P form, while the drift and diffusion terms must be rescaled according to specific rules.

Appendix B. MCS algorithm for Example 3.2

1. Model definition: the OU process ξ_τ is defined on the unit square domain according to **Appendix A** with SDE form: $d\xi_\tau = a(1 - b\xi_\tau)d\xi + cdB_\tau$;
2. Parameter initiation: Given (a,b,c), number of trajectories N_{mc}, number of time steps N_t, absorbing domain [0,1];
3. Time discretization: Set $\Delta\tau = 1/N_t$;
4. Sample initiation: Set $\xi[i] = 0$, $\tau[i] = 0$, $flag[i] = 1$ for $i = 1,\ldots,N_{mc}$;
5. Aging simulation: Set $n = 0$, $\xi_n \triangleq \xi(\tau_n)$

while $n \le N_t$:

Record the aging time $\tau_n = n\Delta\tau$.

Update the degradation by using the Euler–Maruyama method:

$\xi_{n+1} = \xi_n + a(1 - b\xi_n)\Delta\tau + c\sqrt{\Delta\tau}\cdot\delta_n$,

where, $\delta_n \sim N(0,1)$ are independent Gaussian noises.

if $\xi_{n+1} \notin [0,1]$:

Samples absorbed by the boundary.

Set $flag[i] = 0$, $\tau[i] = \tau_n$.

break.

Increase duration time: $\tau[i] = \tau_{n+1}$, $n = n + 1$.

Appendix B (continued)

6. Repeat **Step 5** and obtain $\xi[i], \tau[i], flag[i]$ for $i = 1, \ldots, N_{mc}$;

7. Reliability estimation: $R(t) = \sum_{L_\tau \tau[i] > t} flag[i] \Big/ N_{mc}$.

References

Fan, M., Zeng, Z., Zio, E., Kang, R., & Chen, Y. (2017). A stochastic hybrid systems based framework for modeling dependent failure processes. PloS one, 12(2), e0172680.

Shahraki, A. F., Yadav, O. P., & Liao, H. (2017). A review on degradation modelling and its engineering applications. International Journal of Performability Engineering, 13(3), 299-314.

Paris, P., & Erdogan, F. (1963). A critical analysis of crack propagation laws. Journal of basic engineering, 85(4), 528-533.

Zhang, H., Chen, M., Shang, J., Yang, C., & Sun, Y. (2021). Stochastic process-based degradation modeling and RUL prediction: from Brownian motion to fractional Brownian motion. Science China Information Sciences, 64(7), 171201.

Zhai, Q., & Ye, Z. S. (2017). RUL prediction of deteriorating products using an adaptive Wiener process model. IEEE Transactions on Industrial Informatics, 13(6), 2911-2921.

Wei, Q., & Xu, D. (2014). Remaining useful life estimation based on gamma process considered with measurement error. In 2014 10th International Conference on Reliability, Maintainability and Safety (ICRMS) (pp. 645-649). IEEE.

Ye, Z. S., & Chen, N. (2014). The inverse Gaussian process as a degradation model. Technometrics, 56(3), 302-311.

Iannacone, L., & Gardoni, P. (2024). Modeling deterioration and predicting remaining useful life using stochastic differential equations. Reliability Engineering & System Safety, 251, 110251.

Zhai, J., Dobson, M., & Li, Y. (2022). A deep learning method for solving Fokker-Planck equations. In Mathematical and scientific machine learning (pp. 568-597). PMLR.

He, Z., Wang, S., Shi, J., Liu, D., Duan, X., & Shang, Y. (2025). Physics-informed neural network supported wiener process for degradation modeling and reliability prediction. Reliability Engineering & System Safety, 258, 110906.

Liu, S., Li, W., Zha, H., & Zhou, H. (2022). Neural Parametric Fokker--Planck Equation. SIAM Journal on Numerical Analysis, 60(3), 1385-1449.

Karniadakis, G. E., Kevrekidis, I. G., Lu, L., Perdikaris, P., Wang, S., & Yang, L. (2021). Physics-informed machine learning. Nature Reviews Physics, 3(6), 422-440.

Habibollahi Najaf Abadi, H., & Modarres, M. (2023). Predicting system degradation with a guided neural network approach. Sensors, 23(14), 6346.

Zhou, T., Zhang, X., Droguett, E. L., & Mosleh, A. (2023). A generic physics-informed neural network-based framework for reliability assessment of multi-state systems. Reliability Engineering & System Safety, 229, 108835.

Wang, S., Yu, X., & Perdikaris, P. (2022). When and why PINNs fail to train: A neural tangent kernel perspective. Journal of Computational Physics, 449, 110768.

Zhu, Y., Liu, S., Wei, K., Zuo, H., Du, R., & Shu, X. (2022). A novel based-performance degradation Wiener process model for real-time reliability evaluation of lithium-ion battery. Journal of Energy Storage, 50, 104313.

Sahin, T., von Danwitz, M., & Popp, A. (2024). Solving forward and inverse problems of contact mechanics using physics-informed neural networks. Advanced Modeling and Simulation in Engineering Sciences, 11(1), 11.

Mosleh, A., Al-Sheikhly, M., Chang, Y. S., & Reister, R. (2019). Physics-based probabilistic model of the effects of ionizing radiation on polymeric insulators of electric cables used in nuclear power plants (No. DOE/NEUP-15-8258). Univ. of California, Los Angeles, CA (United States).

Wu, C., Zhu, M., Tan, Q., Kartha, Y., & Lu, L. (2023). A comprehensive study of non-adaptive and residual-based adaptive sampling for physics-informed neural networks. Computer Methods in Applied Mechanics and Engineering, 403, 115671.

Lu, L., Jin, P., Pang, G., Zhang, Z., & Karniadakis, G. E. (2021). Learning nonlinear operators via DeepONet based on the universal approximation theorem of operators. Nature Machine Intelligence, 3(3), 218-229.